

Assessment of tumor microenvironment using DCE MRI and 18Fluoromisonidazole PET imaging in neck nodal metastases

J. F. Jansen¹, H. Schoder¹, N. Lee¹, Y. Wang¹, D. G. Pfister¹, M. G. Fury¹, H. E. Stambuk¹, J. A. Koutcher¹, and A. Shukla-Dave¹

¹Memorial Sloan-Kettering Cancer Center, New York, NY, United States

Introduction

Most malignant tumors develop regions of hypoxia during growth, and usually occur in regions with poor blood perfusion and/or high cell density [1]. The tumor microenvironment in head and neck (HN) cancers plays a critical role in malignant tumor progression and treatment resistance [1]. In particular, tumor hypoxia can cause resistance to radiation- and chemo-therapy, and may promote malignant progression [2]. Gadopentetate dimeglumine (Gd-DTPA)-based dynamic contrast-enhanced magnetic resonance imaging (DCE-MRI) has been suggested to be a useful noninvasive method for characterizing the pathophysiological microenvironment of tumors [3]. With proper compartmental modeling, the data may yield results on tumor-vessel permeability, tumor perfusion, and extracellular-extravascular volume fraction, i.e. data relating to the tumor microenvironment. Targeting hypoxia as a marker of outcome in HN cancer has shown its promises as well as challenges. Radiopharmaceuticals containing nitroimidazole moieties such as ¹⁸F-misonidazole (¹⁸F-MISO) show promise as potential agents for hypoxia imaging [4]. The present study has been designed to compare perfusion and hypoxic status of the neck nodal metastasis in HN cancer using DCE-MRI and ¹⁸F-MISO PET imaging.

Material and Methods

Patients 13 newly diagnosed head and neck cancer patients with metastatic nodes (M/F: 13/0, age: 58±9y, primary cancer: 7 base of tongue, 5 tonsil, 1 larynx) were included. Tumor perfusion and hypoxia was assessed using DCE-MRI and ¹⁸F-MISO PET imaging prior to chemotherapy and radiation therapy. **MRI** MRI was performed on a 1.5 Tesla GE Excite scanner using a 4-channel neurovascular phased-array coil. The protocol consisted of MR imaging covering the entire neck or oral cavity/tongue or larynx using T2-weighted and T1-weighted images. Dynamic perfusion studies were acquired on the nodes using a fast multi-phase spoiled gradient echo sequence. Antecubital vein catheters delivered a bolus of 0.1mmol/kg Gd-DTPA (Magnevist) at 2 cc/s, followed by saline flush. The entire node was covered contiguously with 5-7 mm thick slices, zero gap, yielding 3-6 slices with 3.75-7.5 sec temporal resolution. Acquisition parameters included TR 9 ms, TE 2 ms, flip angle 30°, bandwidth 15.63 kHz, FOV 18-20 cm, time course data points 40-80, and matrix 256x128. **PET** For ¹⁸F-MISO PET imaging, F18-fluoride was produced by the cyclotron by proton irradiation of an enriched O-18 water target in a small-volume titanium chamber. 11.0 mCi of ¹⁸F-MISO was administered by IV and image acquisition at the PET/CT scanner started after 2 hours of the injection. PET/CT images were reconstructed with the standard reconstruction array processor and corrected for attenuation. **Analysis** MRI data was analyzed with IDL 5.4 (Research Systems Inc., Boulder Co). ROIs were manually drawn by an experienced neuro-radiologist. Quantitative DCE-MRI analyses of the tumor tissue time course data was done using the two compartment Tofts model in all ROIs [5], as well as each pixel within the ROI using histogram analysis. A population based arterial input function was used [6]. The latter analyses calculated the pixel K^{trans} (distribution rate constant), v_e (extravascular-extra-cellular volume fraction), and k_{ep} (redistribution rate constant). ¹⁸F-MISO images were transferred to a workstation for image analysis. ¹⁸F-MISO uptake by the tumor was scored: no uptake (score 0) or moderate-severe uptake (score 1), using visual analysis by an experienced nuclear medicine physician. This was followed by the evaluation of CT and PET/CT images. Further semi-quantitative analysis included calculation of tumor-to-muscle ratios as standardized uptake value (SUV) measurements. Whole blood samples collected from each patient were counted in a calibrated multichannel gamma well counter and the blood activity was expressed in as μ Ci/ml, decay corrected to time of injection. Differences in DCE parameters between nodes with ¹⁸F-MISO uptake and nodes without uptake were statistically tested using a 2-sided Student's t-test, with $p < 0.05$. All patients had clinical follow up.

Results and Discussion

For the 13 patients, a total of 17 nodes were analyzed (Table 1). All 17 nodes studied had perfusion and hypoxia data measured by DCE-MRI and ¹⁸F-MISO signal intensity, respectively. Figure 1 displays the results from the two compartment analysis (DCE-MRI) and FMISO uptake (PET) for the right hypoxic node of patient 2. For the nodes that showed no hypoxia on PET imaging (n=7), the mean (\pm SD) values were: ¹⁸F-MISO SUV (1.1 \pm 0.3), K^{trans} (0.33 \pm 0.18), v_e (0.53 \pm 0.23), and k_{ep} (0.66 \pm 0.25). For the nodes that showed moderate to severe ¹⁸F-MISO uptake (n=10) the values were: ¹⁸F-MISO SUV (2.8 \pm 0.8), K^{trans} (0.24 \pm 0.07), v_e (0.61 \pm 0.13), and k_{ep} (0.43 \pm 0.17). A Student's t-test yielded significant lower k_{ep} for nodes with ¹⁸F-MISO uptake ($p=0.042$, figure 2). K^{trans} and v_e were not significantly different in the whole population ($p > 0.1$). Table 1 shows patient 12 to have an extremely low value for v_e (the value is between an interquartile range of 1.5 and 3 [7]), therefore this node can be regarded as an outlier for a subset analysis. This yields significant lower k_{ep} ($p=0.021$) and K^{trans} ($p=0.005$) for nodes with ¹⁸F-MISO uptake. Clinical follow-up information is available over a range of period (6 to 42 months, Table 1).

Conclusion

This initial evaluation of the preliminary result supports the hypothesis that the hypoxic nodes are poorly perfused nodes (lower k_{ep} and K^{trans} values) compared to the nodes that had no hypoxia.

References

[1] Gullledge, Anticancer Res 1996 16:741; [2] Rofstad, Int J Radiat Biol 2000 76:589; [3] Yankeelov, Cur Med Imag Rev 2007 3:91; [4] Van de Weile, Intl J Radiat Oncol Biol Phys 2003 55:5; [5] Tofts, JMRI 1999 10:223; [6] Parker, MRM 2006 56:993; [7] Tukey, Addison-Wesley, Reading, MA. 1977

Subject	Tumor site	Follow Up / Response	Node	FMISO / SUV	K^{trans}	v_e	k_{ep}
1	Tonsil	42 / CR	L	N / 1.0	0.55	0.76	0.73
			R	N / 1.0	0.50	0.69	0.73
2	Tonsil	Deceased	R	Y / 3.2	0.36	0.88	0.41
3	Tonsil	40 / CR	L	Y / 2.0	0.21	0.67	0.31
			R	N / 1.0	0.23	0.51	0.47
4	BOT	35 / CR	L	Y / 2.0	0.27	0.54	0.49
5	BOT	35 / CR	L	Y / 2.1	0.17	0.67	0.26
			R	Y / 2.4	0.20	0.67	0.29
6	Tonsil	26 / CR	R	Y / 2.8	0.29	0.55	0.53
7	BOT	34 / CR	L	Y / 2.6	0.27	0.38	0.76
8	BOT	32 / CR	L	N / 1.0	0.43	0.46	0.92
			R	N / 1.0	0.43	0.44	0.98
9	Tonsil	31 / CR	L	Y / 2.4	0.14	0.62	0.22
10	BOT	22 / CR	L	Y / 4.2	0.24	0.55	0.42
11	BOT	15 / CR	R	Y / 4.2	0.30	0.53	0.61
12	BOT	6 / CR	L	N / 1.0	0.04	0.11	0.40
13	Larynx	10 / NR	R	N / 1.8	0.27	0.75	0.37

Table 1: Patient characteristics and results, BOT: base of tongue. Follow Up (months), CR: complete responder, NR: non-responder, Node: (L: left, R: right), FMISO: uptake (Y: yes, N: no), SUV: standardized uptake value, K^{trans} : distribution rate constant (min^{-1}), v_e : extravascular-extracellular volume fraction, k_{ep} : redistribution rate constant (min^{-1}).

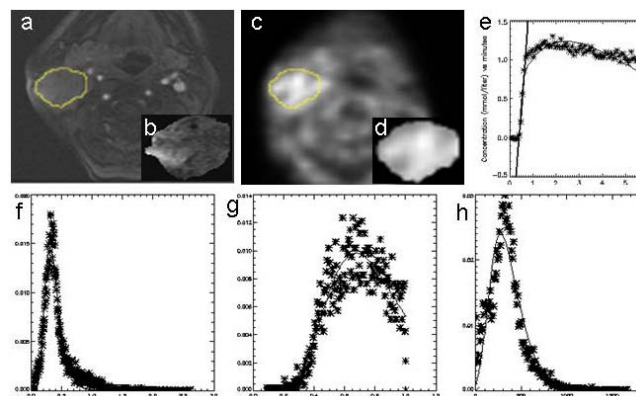


Figure 1: a) Post contrast T1w-image of patient 2 with node outlined in yellow, b) parametric image of the node showing K^{trans} map, c) ¹⁸F-MISO PET image with node marked, d) ¹⁸F-MISO uptake in the node, e) DCE-MRI signal change over time with fit, and histogram distributions for f) K^{trans} , g) v_e , and h) k_{ep} .

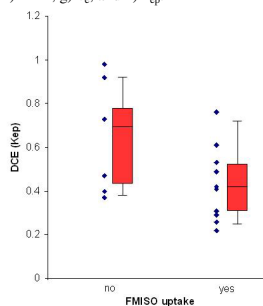


Figure 2: Individual k_{ep} redistribution rate constants (min^{-1}) of the nodes versus the ¹⁸F-MISO PET uptake score (yes or no) for the nodes $p=0.042$. Box-plots are shown in red, displaying minimum, first quartile, median, third quartile, and maximum.